Section A-Research paper

A DETERMINANT OF ZIRCONIUM DOPED COPPER OXIDE NANOPARTICLES AS AN INHIBITOR IN SILANE FUNCTIONALIZED POLYBENZOXAZINE WITH POLYURETHANE COATINGS ABILITY TO ACTIVELY PREVENT CORROSION ON MILD STEEL

N.Valarmathi[1,*] and M.Sivaraju[2]

[1, *]Department of Chemistry, Vivekanandha College of Arts and Sciences for Women (Autonomous), Elayampalayam, Tiruchengode, Tamilnadu, India-637205.

[2] Department of Chemistry, Thiruvalluvar Govt. Arts College, Rasipuram, Tamilnadu, India-637401.

*Corresponding author: valarkumar84@gmail.com

Abstract

The excellent anti-corrosive property of the suggested Polybenzoxazine (Silane functionalized Benzoxazine- Polyurethane- Zirconium doped Copper Oxide Nanoparticles) nanocomposite coating material surfaces opens up new possibilities, to development highly effective non-corrosive coatings for a number of industries. The aggregation of the Polybenzoxazine wrapped Zirconium doped Copper oxide Nanoparticles to the Polyurethane reduce the strength of mild steel because they hindered charge transfer metal as well as electrolyte contact. UV, FT-IR, and XRD techniques were used to initially characterise the created nano-coating materials. In accordance with the findings of the SEM-EDX investigation, the products of corrosion at the surface of the metal electrolyte contact act as an inert conversation that inhibits metal degradation.The Polyurethane film's barrier and mechanical properties are strengthened by the addition of Polybenzoxazine - enhanced Zirconium doped Copper oxide Nanoparticles since Zirconium doped Copper oxide Nanoparticles and

Polybenzoxazine function well together. Also, Thermal Gravimetric Analysis, Differential Thermal Analysis, and Differential Scanning Calorimetric techniques demonstrate that the Zirconium doped Copper oxide Nanoparticles addition increased the copolymer matrix's thermodynamics durability. Then the remarkable corrosion protection capability of coated Polyurethane - Polybenzoxazine - Zirconium doped Copper oxide Nanoparticles was shown by EIS measurements.

Keywords: Doped Nanoparticles, FESEM, FL, PBz, PU, Dip coatings, EIS measurements etc.,

Introduction

As one of the nanotechnology subfields that have received the most attention from academic and industrial research, polymer nanocomposites have proven to be highly effective and multifunctional materials that have a significant impact on our daily lives. When compared to conventional composites and neat polymers, they consistently display an improved combination of mechanical, thermal, optical, and barrier properties[1-3]. The incorporation of nanoparticles can improve the mechanical and physical performance of coatings while also providing numerous special functional features like superhydrophobicity, electroactivity, self-healing capabilities, and others[4-5]. However, a poor match between polymers and inorganic nanoparticles could lead to coating flaws and shorten their useful life[6-7]. This is because when we make a special nanocomposite coating, A group of hydroxyl on the outermost surfaces of the nanoparticles create hydrogen bonds between them, which may have been investigated to encourage nanoparticle aggregation. Significant influences have been employed to explain this problem, comprising physical techniques such as fluid cross-linking, disappear tunnelling, supersonic noises, and chemical-based therapy[8].

The hydroxyl group that exists at the nanoparticles' exterior is effectively removed when

the surface of the nanoparticles is chemically altered, permitting the nanoparticles to move around effectively in composite coatings and increasing their binding capacity to the large quantities of polymers. For these inorganic nanoparticles, organosilanes provide effective surface modifiers. Numberous organofunctional groups, including alkyl, epoxy, and methacrylate amine, may have a detrimental impact on the performance of the finished product[9]. The particle distribution form of the constituent nanoparticles in the tiny materials must therefore be carefully analysed when we create an entirely new nanocomposite coating since it determines whether the coating will exhibit the desired performance or not. Physical techniques like fluid cross-linking, disappear tunnelling, supersonic noises, and chemical-based therapy have been used to overcome this issue to significant impact[10-11].

Corrosion prevention, among other things, is among the main uses of nanocomposite coatings, which is crucial to the growth of the global economy, safety, and conservation[12-13]. Due to their distinctive qualities, which include negligible water absorption, high surface free energy, almost no shrinkage, and superior dielectric characteristics that outperform those of epoxy resins and traditional phenolics, Polybenzoxazine (PBz) has the potential to be related to as corrosion protective coating in the last ten years. Additionally, we created a brand-new PBz precursor (Silane functionalized Benzoxazine) with a silane function and created its polymeric coating (Silane functionalized Polybenzoxazine) using dip coating and the conventional thermal curing method, which demonstrated effective corrosion protection for steels[14-16].

It has been hypothesized that the Silane compounds functionalized the Polybenzoxazine matrix's twofold binding network of PBz and Si-O-Si, as well as its powerful hydrodynamic property and substrate adhesion, serve as an approach for improved corrosion resistance of Silane functionalized Polybenzoxazine coating. Additionally,

during the dip coating procedure, the functionalized energetic alkoxy pairs of silane The hydrolysis of benzoxazine could result in the formation of silanols (SiOH) and its readily establish covalent bonds with the groupsof hydroxyl ion that are found on the outer layer of SiO2 nanoparticles. Without encountering any compatibility issues, it can firmly bind SiO_2 nanoparticles to the Silane functionalized Polybenzoxazine matrix[17].

These features led to the addition of doped nanoparticles to the Silane has been functionalized coating with polybenzoxazine which improved the durability of the coating for the PBz-TMOS(Silane Compound)- Zirconium (Zr) doped Copper oxide (CuO) nanocomposite (PBC) in this study. We present the first physical blending-only PBC coating preparation, which does not undergo any further processing. Nuclear Magnetic Resonance (NMR) Spectroscopy, thermal gravimetric analysis, Fourier Transforms Infrared (FTIR) spectroscopy, thermal gravimetric analysis, and interaction between Silane functionalized Polybenzoxazine and Zr doped CuO nanoparticles. SEM and electrochemical studies in 3.5% aqueous sodium solutions have been used to study the effect of Zr-doped CuO Nanoparticles on Mild Steel's wettability, surface morphology, and corrosion ability.

EXPERIMENTAL

Material and Methods

The following components are used: Copper sulphate, Sodium Hydroxide, Zirconium oxy chloride, ethanol, Paraformaldehyde,4-hydroxy benzaldehyde, (3-aminopropyl)triethoxy silane (APTES), 1,4-dioxane, anhydrous sodium sulphate, ethyl acetae,Polyurethane and double distilled water. The materials were bought in Mumbai, India from Himedia, and Sigma-Aldrich Lab Private Ltd. All the purchased compounds were AR grade which were utilized lacking other extra purification.

General Procedure

Synthesis of Copper oxide Nanoparticles

Using two 500ml beakers, separate solutions of 2.4968M copper sulphate and 0.8M sodium hydroxide were dissolved in each 100ml of distilled water. The copper sulphate is first blended uniformly. The homogeneous mixed solution was then dropped-by-drop combined with sodium hydroxide solution, stirring for 30 minutes at ambient temperature and then 4 hours at 600℃, producing a black precipitate. For 24 hours, this solution was refluxed at room temperature. Then, it was discovered that a translucent solution was sustained at room temperature. The resulting solution was subsequently washed many times with double-distilled water. Finally, the precipitate dried at 120 C. Consequently, an inventory of CuO powdered form was acquired. The aforementioned powder mixture was subjected to heating at 600 C for 4 hours because heat energy can encourage lattice atoms to vibrate and diffuse for crystallization.

Synthesis of Zirconium Doped Copper Oxide Nanoparticles

Each 100 ml of distilled water was independently dissolved using three 500 ml beakers to create an identical molar (2.4968 M) solution of copper sulphate, different concentrations (0.01% and 0.02%) of zirconium oxychloride, and 0.08 M of NaOH. First, homogenous mixtures of zirconium and copper sulphate solutions were made. After stirring for 30 minutes at ambient temperature and then for 4 hours at 600^0C, NaOH solution was then added dropwise to the homogeneous mixed solution, producing a black precipitate. At room temperature, this solution was refluxed for 24 hours. The result was then a clear solution that was discovered to be stable at room temperature. Following that, the solution rinsed with double-distilled water many times. At 120^0C, the precipitate was finally dried. Zr doped CuO sample was so obtained. This sample was heated to 600^0C for 4 hours in an annealing process because heat energy

can increase the vibration and diffusion of atoms in the lattice, which is necessary for crystallisation.

Synthesis of Monomer (Benzoxazine Monomer)

The chloroform-dissolved 4-hydroxybenzaldehyde, Triethoxysilyl propylamine, and paraformaldehyde were added to a fixed water condenser in an R.B. flask for 16 hours. The resultant mixture was extracted with ethyl acetate when the reaction was complete, and then it was washed in 0.1N base solution, water, and salinity solution. An analysis of thin-layer chromatography was conducted to determine whether the reaction had been completed.With the aid of a separating funnel and an anhydrous sodium sulphate solution, the organic layer was removed and dried[18]. FT-IR, UV-Visible, and NMR spectrum methods were used to characterize the pale yellow oil that I eventually collected which was named as monomer (Bz).

Techniques of Dip Coating

The generated Monomer (Bz) is dissolved in 1,4-dioxane together with two different Zr doped CuO nanoparticle concentrations (0.01% and 0.02%). It has been discovered that the reaction mixture contains Polyurethane adhesive. Three distinct Polybenzoxazines and Polyurethanes with silane functionalization, as well as 0.01% and 0.02% Zr doped CuO nanoparticles, have been assembled. The mild steel rod was cleaned with acetone, trimethylamine, and water. To enhance adhesion, Emery paper was used to polish the mild steel (MS). The MS was then submerged for 1 minute in TEOS-PBz:PU:% of doped nano solutions, and the cleanup process took about 1 minute[19]. Finally, the covered mild steel was successfully heated and treated in the furnace for three hours at 200 °C. Additionally, thermal gravimetric analysis and electrochemical impedance investigations have been used to analyze the dipping MS.

Scheme

SCHEME: SYNTHESIS AND FORMATION OF SILLANE FUNCTIONALIZED POLYBENZOXAZINE ZR DOPED CUO NANOPARTICLES WITH POLYURETHANE

RESULTS AND DISCUSSION

INTERPRETATION OF CuO NANOPARTICLES AND Zr DOPED CuO NANOPARTICLES

Uv-Visible Spectroscopic Techniques

For pure CuO, the UV-Vis absorption spectrum's peak is located at 3389 cm-1. With varying concentrations of 0.01% and 0.02%, the UV-Vis absorption spectra of Zr doped CuO NPs also show significant sharp peaks at 351.2 nm and 378.4 nm. For Zr doped CuO NPs, It is seen that the absorption spectra's location shifts to the lower wavelength side. This suggests that the doping of Zr ions widens the band gap between CuO materials. The Burstein-Moss effect can be used to explain the widening of the band gap or blue shift. While the band gap value increases and the Fermi level changes close to

the low energy transactions are stopped.Figure 1(a-c) illustrates the band gaps for pure CuO and Zr (at various concentrations of 0.01% and 0.02%) doped CuO, respectively, which are 3.1 eV, 2.58, and 2.75 eV. The band gap of Zr doped CuO NPs somewhat increases when compared to pure CuO NPs. This also fits well with the quantum confinement effect of nanoparticles.

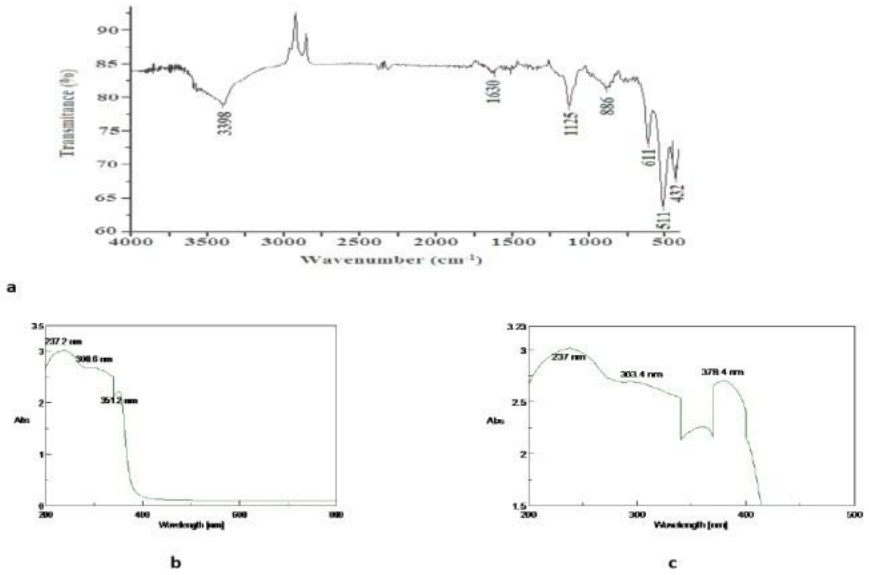

FIGURE 1 (a-c) BAND GAP MEASUREMENT FOR CUO NPS, Zr (0.01%) DOPED CUO NPS AND Zr(0.02%) DOPED CUO NPS

FT- IR Spectroscopic Studies

Figure 2 displays the synthesized CuO and Zr doped CuO NPs' FT-IR spectra at various concentrations (0.01%, 0.02%). Broad absorption bands at 3509 nm, 3536 nm, and 3521 nm are found at the hydroxyl groups of absorbed water molecules or CuO for undoped and Zr doped CuO NPs with varying concentrations (0.01% & 0.02%), respectively. For the pure CuO NPs and the Zr (0.01%, 0.02%) doped CuO NPs, the symmetric C-O bands are seen at 1232 and 1239, 1225 nm, respectively. For undoped and doped CuO samples, the C-H out-of-plane bending bands can be seen at 673, 681, and 692 nm, respectively. For each CuO NPs, the Cu-O stretching bands are seen at 544, 551, and 560 nm.

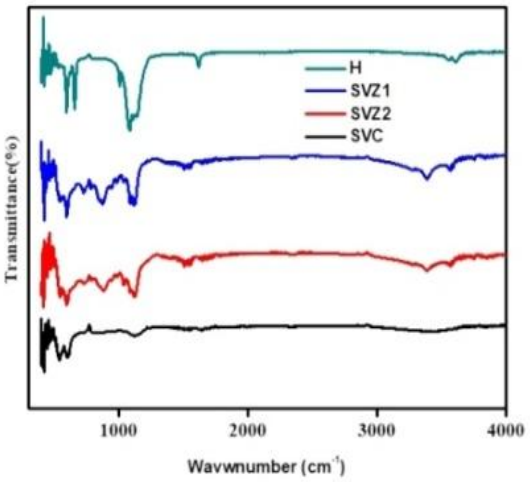

FIGURE (2) FT-IR ABSORPTION SPECTRA OF STANDARD, CUO NPS, Zr (0.01%)DOPED CUO NPS AND Zr (0.02%) DOPED CUO NPS.

X-Ray Diffraction Studies

The pure CuO NPs have very weather-like structures, as evidenced by the sharp and powerful diffraction peaks. For the pure CuO NPs, the standard diffraction peaks (Space group: P63mc) depict the Wurtzite's hexagonal type of structure which is confirms from JCPDS data (361451). However, doping Zr yields no further peaks (Figure 3), indicating no movement in the development of impurity phases. Compared to the pure CuO sample, the peaks of the Zr-doped CuO sample show a very small shift. This change also reflects the strain brought on by the substitution of Zr with each combination, which is a consequence of the implications of the ionic radii of the various metal ions. Scherer's equation, written as D= KDCOS The wavelength of the radiation (1.5406 for CuK), the peak location, the peak width at half-maximum intensity, the peak size in nanometers, the peak location, the wavelength of the radiation, and the X-ray line broadening approach are used to determine the particle grain size of pure CuO Nps.

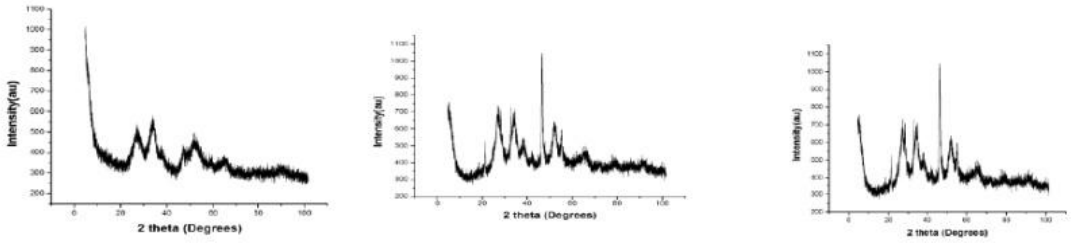

FIGURE 3 (a-c) XRD PATTERN OF PURE CUO NPS, Zr(0.01%) DOPED CUO NPS AND Zr (0.02%) DOPED CUO NPS

Energy Dispersive Analysis X-ray Studies

Energy Dispersive Analysis X-ray spectroscopy or, EDAX was utilised to interpret the chemical makeup of recently synthesised doped nanoparticles. Figure 4 displays the Zr doped and undoped CuO NPs' EDAX spectra. Zr, O, and Cu concentrations in the doped materials have been identified as 20, 36, and 42%, respectively.

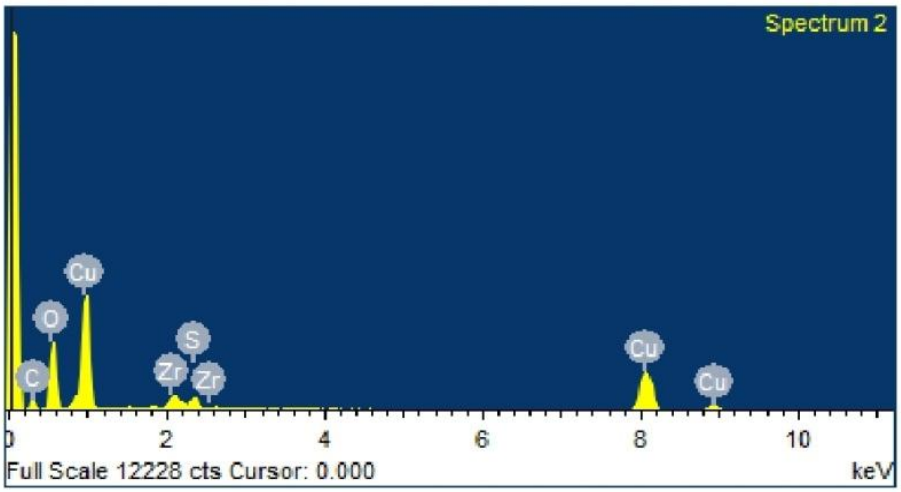

FIGURE (4) EDAX Spectra of Zr doped CuO Nps

Field Emission scanning Electron Microscopic analyses

The typical size of the crystallite associated with pure CuO NPs is discovered to be 25

nm. such typical crystallite size decreases in Zr-doped CuO NPs. Foreign pollutants, particularly La, inhibit the development of nuclei and the ensuing development rate of CuO NPs. are the principal cause of the reduction in particle size in the host CuO lattice. Figure 5 shows the FESEM picture of the unpolluted CuO, and Zr-doped CuO nanoparticles. The photos demonstrate the amorphous, feather-like shape of the pure CuO and Zr doped CuO nanoparticles. In comparison to pure CuO NPs, the widths of the spherical size are observed to be reduced; measuring 25 nm for Zr doped CuO NPs. The host material that incorporates the Zr metal ion in the CuO NPs surface area has distorted, which is the cause of the decrease in width size. As a result, Zr doping reduces the diameters of CuO NPs.

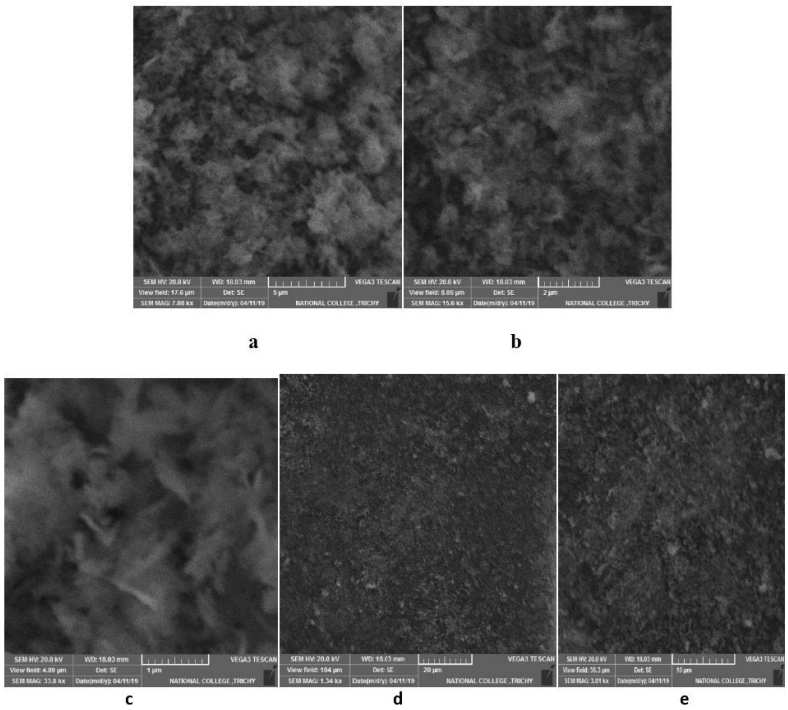

FIGURE 5(a-e) FESEM IMAGES OF PURE CUO AND Zr DOPED CUO NPS

Fluroluminescence Study

It was more foreseeably that CuO nanopowders would have distinctive emission peaks with various shapes. Figure 6 depicts the photoluminescence spectra of cubic CuO and

doped Zr nanoparticles stimulated between 310 and 314 nm. There were clearly visible emission peaks at 346 nm (UV), 398 nm (weak blue), 468 nm (weak blue green), 482 nm (green), and 570 nm (red). The transition between $^2F_{5/2}$ 5d and $^2F_{7/2}$ 5d was blamed for the sharp peak at 398 nm. The transition of charge from CuO's band of 4f to its valence band was reported to cause two emission peaks at 380 and 422 nm, and the emission of defects caused by oxygen vacancies implied the presence of Cu2+ in the CuO sample. As a result, the emission has peaks between 320 and 800 nm, and cerium ions are trivalent.

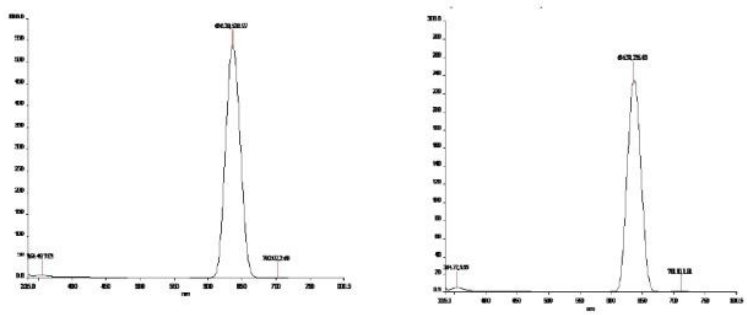

a b

FIGURE 6 (a-b) FL EMISSION SPECTRA OF PURE CUO NPS AND ZR DOPED CUO NPS

CHARACTERIZATION OF MONOMER AND POLYMER NANOCOMPOSITES

UV Studies

The UV-Vis retention range of Monomer and sillane functionalized Polybenzoxazine-Zr-doped CuO NPs at room temperature, at various times, is shown in Figure 7. Two retention tops, one for the development of the Polybenzoxazine ring and the other for the transformation of the C=C paraformaldehyde moiety, have been seen at 329 and 281 nm, respectively. The peak's top at 329 nm decreases while the force at 281 nm increases after the creation of sillane functionalized Polybenzoxazine -PU with

Zr-doped CuO nanocomposites at various time intervals. This behaviour proved conclusively that the Polybenzoxazine retain a generated fragment that can be converted into a photodimerization response when exposed to light. Each of the aforementioned findings that suggested an efficient union of the Polybenzoxazine has a corresponding[20].

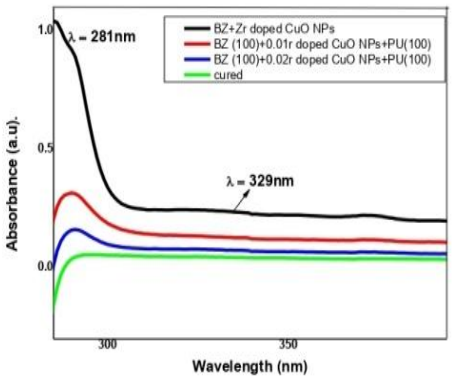

FIGURE (7) UV CHARACTERIZATION OF PURE AND SILANE FUNCTIONALIZED POLYBENZOXAZINE-PU - Zr DOPED CUO NPS AT VARIOUS MEDIUM

FT-Infrared Studies

The Monomer exhibits FT-INFRARED technique in figure 8a (KBr): 2942 cm^{-1} (Aliphatic C-H vibrations) 1687 cm^{-1} (stretching C=O), 1601 cm^{-1} (frequency stretching CH=N), 1318 cm^{-1} (W-CH_2 oxazine ring), 1238 cm^{-1} (asymmetric of C-O-C stretching), 1118 cm^{-1} (asymmetric of C-N-C stretching), 1031 cm^{-1} (C-O-C symmetric bond in oxazine ring) and In figure 8b exhibits FTIR spectra of sillane functionalized Polybenzoxazine /PU with Zr-doped CuO nanocomposites, the benzoxazine situated around 1647 cm^{-1} compares to C=C ,C=O, and NH holding, Polybenzoxazine possesses aromatic amino gatherings that have been demonstrated to exist. The wide top at 3002-3500 cm^{-1} was doled out to NH & OH extending modes coming about because of sillane functionalized Polybenzoxazine -PU with Zr-doped CuO nanocomposites[21-22]. The FTIR spectra of sillane functionalized Polybenzoxazine /PU with Zr-doped CuO nanocomposites contain the benzoxazine attributes of both Zr-doped CuO NPs and PBz.

This confrms that the Zr-doped CuO nanoparticles are modifed by Polybenzoxine.

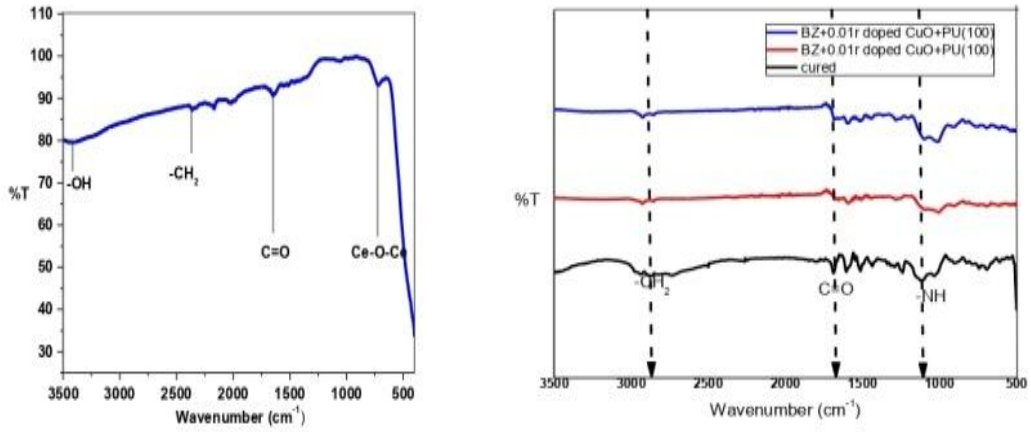

FIGURE 8 (a-b) FT-IR CHARACTERIZATION OF PURE AND SILANE FUNCTIONALIZED POLYBENZOXAZINE-PU - Zr DOPED CUO NPS AT VARIOUS MEDIUM

Xrd Studies

The XRD analysis of PBz/CeO2 and Zr-doped CuO nanoparticles is shown in Figure 9. The diffraction edges for the PBz/Zr-doped CuO nanoparticles test and the tests using Zr-doped CuO nanoparticles are at 28.6, 33.2, 47.5, 56.4, 59.1, 69.4, 77.0, and 79.1 degrees, respectively. It is highly compatible with Zr-doped CuO nanoparticles in cubic fluorite structure (JCPDS No. 34-0382). The encasing of PBz over the surface of the Zr-doped CuO nanoparticles is confirmed by the XRD study. The trademark top, however, virtually follows the same example as Zr-doped CuO nanoparticles with low force and no shift was seen due to PBz/Zr-doped CuO nanoparticles. The Zr-doped CuO nanoparticles' design has not been destroyed, and the arrangement of PBz has taken place on their outer layer, as evidenced by the reduced force without any recognisable shift in tops[23-26].

The size of approximate particles range were predictable from usage of Scherer's formula ($D = 0.9 \times \lambda / \beta\cos\theta$, Where β is the Full-width half maxima (FWHM) of the

most intense peak; θ is Bragg's diffraction angle for the most peak (111), D is an average particle size; λ is the wavelength of the radiation i.e., 1.5406 Å for Cu Kα radiation; k is shape factor which is equal to 0.89;, the analysed particle size was found to be 8.61 nm.

The XRD studies produced for the PU, PU- PBz-Zr(0.01%)-doped CuO nanoparticles, and PU- PBz / Zr(0.02%)-doped CuO nanoparticles coatings submerged in chloride media for 5 days are shown in Fig. 9, respectively. PU, PU-PBz-Zr(0.01%)-doped CuO nanoparticles, and PU-PBz/Zr(0.02%)-doped CuO nanoparticles covering the mild steel surface are seen and assessed by XRD for the development of corruption items. Additionally, Figure 9 displays the XRD patterns for the PU, PU-PBz-Zr(0.01%)-doped CuO nanoparticles, and PU-PBz/Zr(0.02%)-doped CuO nanoparticles coatings upgraded tops obtained for both -Fe-O and Fe_3O_4. This revealed that the consumption interaction occurred quickly for PU-covered mild steel.

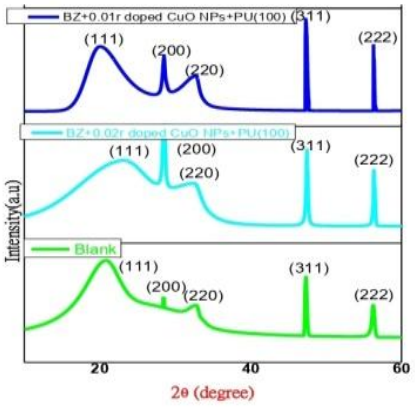

FIGURE (9) XRD PATTERN OBTAINED FOR PU, PU- PBz-Zr(0.01%)-DOPED CUO NANOPARTICLES, AND PU- PBz / Zr(0.02%)-DOPED CUO NANOPARTICLES COATINGS SUBMERGED IN CHLORIDE MEDIA FOR 5 DAYS

Sem with Edax Studies

The surface morphology and natural component of Zr-doped CuO nanoparticles and PBz/Zr-doped CuO nanoparticles used SEM/EDX to investigate, as exposed in Figure

10 a and b. SEM images of the Zr-doped CuO nanoparticles revealed a round form, as is typical for this type of nanoparticle. The SEM/EDX analysis validates the surface modification of Zr-doped CuO nanoparticles helped polybenzoxazine. The SEM/EDX analysis has demonstrated that O, Zr, and Cu are present in the PBz/Zr-doped CuO nanoparticles.

Mild steel coated with Polyurethane, PU- PBz-Zr(0.01%)-doped CuO nanoparticles, and PU- PBz/Zr(0.02%)-doped CuO nanoparticles and its cross-sectional morphologies, after 5 days of immersion in a solution of sodium chloride, are shown in Figures 10c and 10d. The formation of a more uniform layer on soft steel in the presence of PU-PBz/Zr(0.02%)-doped CuO nanoparticles confirmed the absence of Zr-doped CuO nanoparticles collection and the considerable scattering in the covering. Due to the PU covering, breaks with consumable products were seen to exist. Less of the important items were acknowledged, and it was established that PU-PBz-Zr(0.01%)-doped CuO nanoparticles and PU-PBz/Zr(0.02%)-doped CuO nanoparticles coating offered the best protection against PU coating erosion. When compared to other films that are reliable with diverse results from numerous evaluated methods, the utilisation of PBz/Zr-doped CuO nanoparticles in the PU covering provided better efficiency assurances. The protective coating made of PU-PBz/Zr(0.02%)-doped CuO nanoparticles exhibits a modest increase in utilisation rate over time due to the buildup of crumpled metal at the steel combined place. According to the problems of the EDX, Cu, Zr, and O are accessible in the enhanced integrity structures. The primary Defending against corrosion is an important part of corrosion prevention properties of PBz -PU /Zr(0.02%)-doped CuO nanoparticles covered mild steel is strengthening reactive metals comprising Cu, Zr at scratch. The EDX investigation shows that the Cu, Zr, and O devaluation components are unquestionably progressed and impede the ingestion start-up process.

Therefore, it is expected that the nanoscale thin film and the consuming component coatings made up of Cu, Zr, and O that are enclosed at the metal/covering point of interconnection may enhance the coated mild steel's exceptional corrosion resistance.

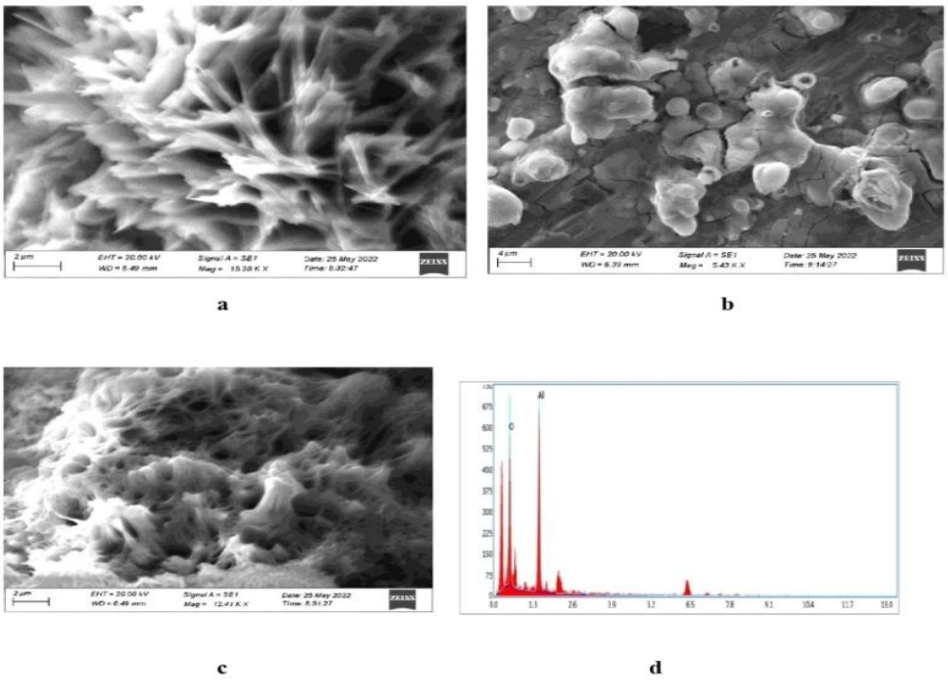

FIGURE 10 (a-d) SEM WITH EDAX OBTAINED FOR PU, PU- PBz-Zr(0.01%)-DOPED CUO NANOPARTICLES, AND PU- PBz / Zr(0.02%)-DOPED CUO NANOPARTICLES COATINGS IN CHLORIDE MEDIA FOR 5 DAYS

EIS STUDIES

The metal surface/solution and coating/solution interfaces are shown in the EIS data. The impedance response of the Polyurethane resin, Polybenzoxazine-Zr-doped CuO nanocomposite material and the uncoated MS substrate is depicted as a Nyquist plot in Fig. 11(b). Low frequency interception was blamed on the resistance to a charge transfer at the risk of corrosion. The charge transfer resistance and double-layer capacitance were computed from the EIS measurement, and the outcomes are shown in Table 1. The charge transfer resistance values of the mild steel substrate and blank acrylic resin were many orders of magnitude lower than those of the PU-Zr-doped CuO and PU/mild steel materials. In particular, the PU-Zr-doped CuO nanocomposite coating on the substrate

of mild steel shows better corrosion resistance than the bare substrate, as shown by increased charge transfer resistance and a decrease in double-layer capacitance.

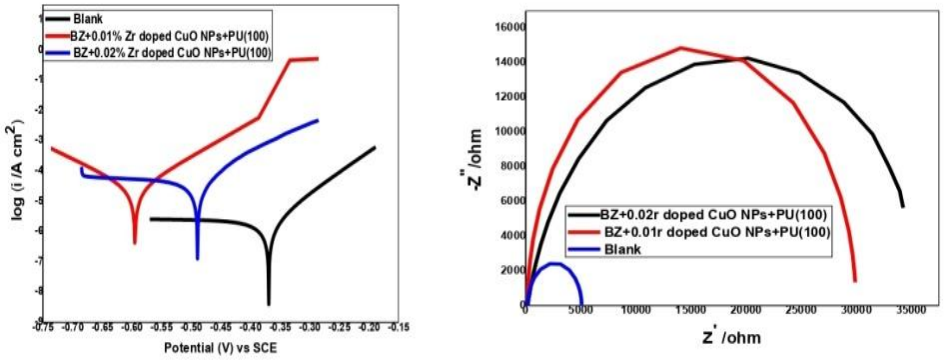

a b

FIGURE 11 ELECTROCHEMICAL BEHAVIOR OF (a) TAFEL POLARIZATION OF MONOMER AND SILANE FUNCTIONALIZED POLYBENZOXAZINE –Zr DOPED CUO NCS ON MILD STEEL IN 3.5 NACL FOR 5 DAYS (b) NYQUIST PLOT OF MONOMER AND SILANE FUNCTIONALIZED POLYBENZOXAZINE –Zr DOPED CUO NCS ON MILD STEEL IN 3.5 NACL FOR 5 DAYS

Fig. 11 a shows the electrochemical polarisation curves for uncoated and coated MS. The graph compares the corrosion resistance behaviours of MS that has not been coated with anything to MS that has been coated with PU-Zr-doped CuO nanocomposite and pure Polyurethane materials. The Tafel extrapolation method was used to derive the parameters of corrosion such as risk of corrosion, current of corrosion, and peaks of Tafel anodic/cathodic. Table 1 displays the computed corrosion rates (rcorr). The data unambiguously show that polybenzoxazine at Zr-doped CuO nanocomposites improve corrosion resistance. The MS substrate coated with 100% Polybenzoxazine- Zr-doped CuO nanoparticles showed the greatest Noble corrosion potential shifts to a positive state compared to the other coated samples. This shows that corrosion resistance was improved when more Zr-doped CuO nanoparticles with Bz nanocomposite coating was present. This might be because the hydroxyl ions and massive Cu cations, which have a positive charge, bond together readily and form a sturdy bilayer via surface of the MS substrate. This slows down the transmission of charges between the coated substrates

and the environment outside.

S. NO.	Sample of Concentrations (PBz:PU:Doped Nano)	Report of Tafel				Report of Nyquist Plot		
		I_{corr} (uA)	E_{corr} (mV)	Efficiency of Corrosion (%)	Rate of Corrosion	R_{ct} (ohm)	C_{dl} (F)	Efficiency of Inhibition (%)
1	Monomer	0.041	-491.761	-	488.431	2.814	0.3917	-
2	100:100:0.01% Doped nano	0.020	-593.579	41.09	298.350	423.6	48.48e-6F	98.95
3	100:100:0.02% Doped nano	0.001	-365.467	94.23	24.258	1376	8.577e-6F	99.89

Table -1. Electrochemical behavior of monomer and silane functionalized polybenzoxazine –zr doped cuo NCs on MS in 3.5% of Nacl for 5 days immersion at different concentrations

100% Polybenzoxazine- Zr-doped CuO Nanocomposite-coated MS exhibits a corrosion rate of 3.851102 mm which is about 21 times litter than the corrosion rate of the uncoated MS substrate (8.432 101 mm). The blockage of the cathodic sites is thought to be the cause of MS's increased corrosion resistance in the presence of copper. Copper ions precipitate insoluble copper hydroxide/copper oxide at local regions by forming islands, acting an energetic site of cathodic inhibitors. The islands obstruct the sites of cathodic, which lowers the current of cathodic and lowers the overall corrosion rate.

TGA and DTA, DSC Studies

Polymeric materials change from the substances of hard glassy to the substances of soft rubbery at the glass transition temperature (Tg). In order to calculate a material's Tg, we

need to examine the segmental mobility and crosslink density of the material. As a result of hydrogen bonding between the phenolic hydroxyl groups in polybenzoxazine, it has a higher Tg.TGA analysis in a nitrogen environment was used to assess the thermal stability of coatings. Figure 12 displays the outcomes.

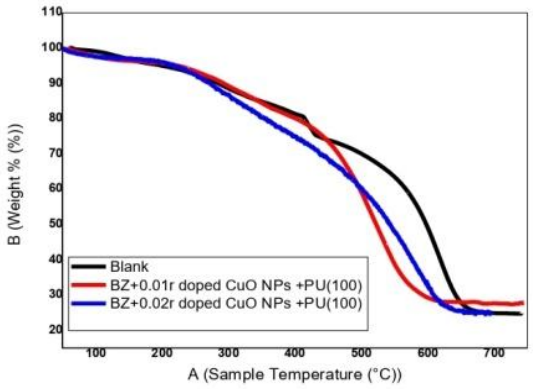

FIGURE (12) TGA STUDIES OF MONOMER AND SILANE FUNCTIONALIZED POLYBENZOXAZINE –Zr DOPED CUO NCS ON MILD STEEL IN 3.5 NACL FOR 5 DAYS AT DIFFERENT CONCENTRATIONS

The result was a decrease in coating weight as a function of temperature. Table 2 shows the 5 weight percent (Td 5%), 30 weight percent (Td 30%), and residual weight percent (char yield) loss degradation temperatures at 580-600°C. According to Fig., PBz/PU with Zr-doped CuO NPs coatings outperform Polybenzoxazine coatings up to 250°C. While the Polybenzoxazine coating deteriorates by 15%, the PBz/PU coatings deteriorate by less than 10%. This is due to the Polyurethane have high cross-linking density. The increases of the coating cross-linked density as the content of Polyurethane increases, and the coating has high thermal stability between 500°C and 562°C. Table 2 shows that as the urethane percentage increases, so does the coating of the thermal stability. As a result, coatings containing more urethane had higher crosslink density than coatings containing only Polybenzoxazine. A polymer's heat stability can be increased by limiting chain mobility and increasing cross-linking density. Because the

Polyurethane segment produced significantly less char than the polybenzoxazine segment, the char yield of the Bz/PU coating system decreased. The heat-resistance index (THRI) is calculated using the equation below.

$$T_{HRI} = 0.49 \text{ X } [T_5 + 0.6 \text{ x } (T_{30} - T_5)]$$

Figure 13 and Table 2 demonstrate the DTA thermal grammes of PU@PBz Zr-doped CuO nano cured coatings with varying molar ratios. It was discovered that as the molar concentration of urethane moiety rose, the Tg of the cured coating changed towards higher temperatures.

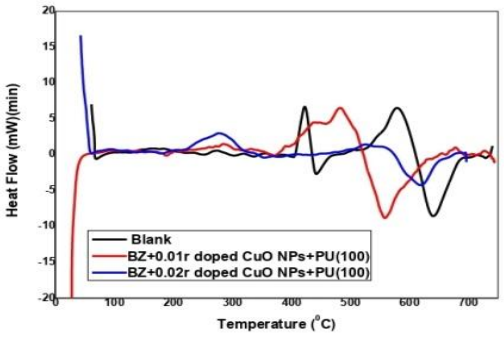

FIGURE (13) DTA STUDIES OF MONOMER AND SILANE FUNCTIONALIZED POLYBENZOXAZINE –Zr DOPED CUO NCS ON MILD STEEL IN 3.5 NACL FOR 5 DAYS AT DIFFERENT CONCENTRATIONS

S.NO.	Coating materials	Temperature of Onset (°C)	Temperature of Offset (°C)	Td^5 (°C)	Td^{30} (°C)	T_{HRI}
1	Monomer	88.38	540	150.24	300.01	115.17
2	100:100:0.01% Doped nano	202.50	565	296.91	413.81	166.04
3	100:100:0.02% Doped nano	213.89	592	279.13	421.16	172.67

Table-2 TGA tabulation of monomer and silane functionalized Polybenzoxazine –Zr doped Cuo NCs on MS in 3.5% Nacl for 5 days immersion at different concentrations

It is evident from the DSC thermogram of monomer (Bz) that one peak corresponds to the crystallization temperature of the monomer (Bz), and two peaks correspond to the melting temps of the monomer (Bz), which are answerable for the opening of the PBz rings.The thermograms of PU-PBz@ Zr (0.01%)-doped CuO NCs reveal two exothermic peaks at 423℃ and 517℃, respectively. It also exhibits two endothermic peaks at 460℃ and 578℃. The initial exothermic peaks for PU (100): PBz@ Zr(0.02%)-doped CuO NCs, which are answerable for opening of ring cause the Polyurethane's cross-linking capacity, occur between 440°C and 521°C. The melting of the PU-PBz@ Zr (0.02%)-doped CuO NCs causes the second endothermic peak at 468°C, 580°C. Bz, PU/ PBz@ Zr(0.01%)-doped CuO NCs, and PU/ PBz@ Zr(0.02%)-doped CuO NCs had Tg values of 252°C, 363°C, and 369° C, respectively. Because of the cross-linking feature of PU, It is obvious that coatings with more PU will be more thermally stable. Comparatively, to Polyurethane alone, benzoxazine monomer increases the resistance of thermal. (benzoxazine monomer), according to DSC data (Table 3 & Figure 14).

S.NO.	**Coating materials**	**Tg (°C)**	**$T_{(onset)}$ (°C)**	**Exo T_{peak} (°C)**	**Endo T_{peak} (°C)**
1	Monomer	252	238	454	531 551
2	100:100:0.01% Doped nano	363	328	423 517	460 578

3	100:100:0.02% Doped nano	369	331	440 521	468 580

Table-3 DTA tabulation of monomer and silane functionalized polybenzoxazine –zr doped cuo NCs on MS in 3.5% Nacl for 5 days immersion at different concentrations

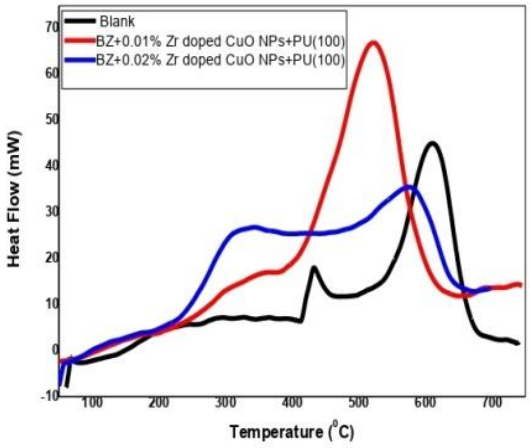

FIGURE (14) DSC STUDIES OF MONOMER AND SILANE FUNCTIONALIZED POLYBENZOXAZINE –Zr DOPED CUO NCS ON MILD STEEL IN 3.5 NACL FOR 5 DAYS AT DIFFERENT CONCENTRATIONS

CONCLUSION

At first Zr-doped CuO Nanoparticles (Inhibitor) provides a high yield, a time-saving procedure, and is environmentally benign which characterization studies are carried out utilising UV, XRD, EDAX, FE-SEM, FTIR, and FL. Each and every piece of data agrees with the allotted structures. According to the current state of the artistic endeavours, Silane functionalized PBz-PU- Zr-doped CuO nanocomposites that have been effectively deposited on a mild steel exterior, and tests using FTIR, TGA, DTA, DSC, EIS, and SEM/EDX revealed that Zr-doped CuO nanoparticles were formed and arranged in layers in the polymerization. The coating's consistency in thickness and lack of cracks made it an outstanding corrosion-resistant compound under saltwater

conditions, which is how it became recognised. As a result, the mild steel that had been coated with Silane functionalized PBz- PU- Zr-doped CuO was less corroded and had a distinct surface structure with a somewhat rougher interface. According to electrochemical studies, increasing the dimension of the absorbed layer increases the resistance of charge transfer (Rt), decreases the capacitance of double layer (Cdl), and improves corrosive current (Icorr) values. According to AC resistance tests, the presence of the Silane functionalized PBz- PU- Zr-doped CuO coating material considerably affected the mild steel layer's treatment interaction by establishing a protective layer. Fluid interaction distances were used to demonstrate the ultrahigh hydrophobic properties. For mild steel utilised in commercial cooling water systems, the Silane functionalized PBz- PU- Zr-doped CuO coating method containing Silane functionalized PBz showed more successful at resisting rust than Zr-doped CuO. It may open up new possibilities for the usage of coastal engineering components that are susceptible to seawater-induced accelerated deterioration.

ACKNOWLEDGMENTS

We (Authors) happy to convey thankfulness to Dr. P. Shanmugasundaram, Head, Department of Chemistry, Thiruvalluvar Govt. Arts College, Rasipuram, India and Mrs.K.Jayanthi, AP/Chemistry, Queen Mary's College, Chennai, India for their continuous carrying and suggestions of this work completion.

CONFLICT OF INTERESTS

Authors declare no conflict of interest.

AUTHOR CONTRIBUTIONS

N.Valarmathi: Laboratory work, Analysis process, Full paper writing process.

M. Sivaraju: Initiate the work Process, Guideline& Evaluation, Full paper Review.

N.Valarmathi https://orcid.org/0000-0003-2541-902X

M. Sivaraju https://orcid.org/0000-0001-8502-5458

REFERENCES

1. Eds. Scharnweber, N. Y. Abu-Thabit and A. S. H. Makhlouf, In Handbook of Nanoceramic and Nanocomposite Coatings and Materials, *Butterworth-Heinemann*, **24**, 515−549 (2015).
2. T. Agag and T. Takeichi, *Polymer*, **52**, 2757-2763 (2011), https://doi.org/10.1016/j.polymer.2011.04.044.
3. H. Deng, L. Lin, M. Ji, S. Zhang, M. Yang and Q. Fu, *Progress in Polymer Science,* **39** (4), 627-655(2014), http://dx.doi.org/10.1016/j.progpolymsci.2013.07.007.
4. R.Bayan and N. Karak, *Composites Part A Applied Science and Manufacturing*, **110**, 142−153, (2018), https://doi.org/10.1016/j.compositesa.2018.04.024.
5. F. Zhang, L. Zhao, H. Chen, S. Xu, D. G. Evans and X. Duan, *A Journal of the German Chemical Society*, **47**, 2466−2469, (2008), https://doi.org/10.1002/anie.200704694.
6. S.L.Bee, M.A.A.Abdullah, S.T.Bee, L.T. Sin and A.R.Rahmat, *Progress in Polymer Science,* **85**, 57−82, (2018), https://doi.org/10.1016/j.progpolymsci.2018.07.003
7. E. I. Akpan, X. Shen, B. Wetzel and K. Friedrich,, In Polymer Composites with Functionalized Nanoparticles, *Elsevier*, **2**, 47−83, (2019).
8. T. Ribeiro, C. Baleizaõ and J.Farinha, *Materials*, **7**, 3881−3900, (2014), https://doi.org/10.3390/ma7053881.
9. S. Ammar, K. Ramesh, I. A. W. Ma, Z. Farah, B. Vengadaesvaran, S. Ramesh and A. K. Arof, *Surface and Coatings Technology*, **324**, 536−545, (2017),

https://doi.org/10.1016/j.surfcoat.2017.06.014.

10. M. J. Palimi, M. Rostami, M. Mahdavian and B. Ramezanzadeh, *Applied Surface Science*, **320**, 60− 72 (2014), http://dx.doi.org/10.1016/j.apsusc.2014.09.026.
11. M. J. Palimi, M. Rostami, M. Mahdavian and B. Ramezanzadeh, *Progress in Organic Coatings*,**77**, 1935−1945 (2014), http://dx.doi.org/10.1016/j.porgcoat.2014.06.025.
12. E. B. Caldona, A. C. C. De Leon, P. G. Thomas, D. F. Naylor, B. B. Pajarito and R. C. Advincula, *Industrial and Engineering Chemistry Research*, **56**, 1485−1497, (2017), https://doi.org/10.1021/acs.iecr.6b04382.
13. Y. Torknezhad, K. Khosravi and M. Assefi, *Material Corrosion*, **69**, 472−480,(2018), https://doi.org/10.1177/8756087918806027.
14. H. Dong, Z. Xin, X. Lu and Y. Lv, *Polymer*, **52**, 1092–1101, (2011), https://doi.org/10.1016/j.polymer.2011.01.009
15. L.Qu and Z.Xin, *Langmuir*, **27**,8365–8370, (2011), https://doi.org/10.1021/la200073v.
16. C. Zhou, X. Lu, Z. Xin and J. Liu, *Corrosion Science*, **70**, 145–151, (2013), http://dx.doi.org/10.1016/j.corsci.2013.01.023.
17. C. Yan, X. Fan and J. Li, *Journal of Applied Polymer Science*, **120**, 1525–1532, (2011), http://dx.doi.org/10.1002/app.33383.
18. H. Deng, L. Lin, M. Ji,; S. Zhang,; M. Yang and Q. Fu, Progress in Polymer Science, **39** (4), 627-655, (2014), http://dx.doi.org/10.1016/j.progpolymsci.2013.07.007.
19. Changlu Zhou, Xin Lu, Zhong Xin and Juan Liu, *Corrosion Science*, **80,** 269-275 (2014), http://dx.doi.org/10.1016/j.corsci.2013.11.042.

20. N. Srinivasa Rao, V.Mandava and Basaveswara Rao, *American Journal of Materials Science*, **5**(3): 66-68, (2015), doi:10.5923/j.materials.20150503.02.
21. K. Nithya, P. Yuvasree, N. Neelakandeswari, N. Rajasekaran, K. Uthayarani and M. Chitra, In Proceedings with International Conference on Materials and Characterization Techniques, *International Journal of Chem Tech Research*, **3**, 2220-2222, (2014), CODEN (USA): IJCRGG ISSN : 0974-4290
22. K. Phiwdanga, S. Suphankija, W. Mekprasarta and Wisanu, *Energy Procedia*, **34**, 740-745, (2013), doi:10.1016/j.egypro.2013.06.808.
23. Peter Djinovic, Jurke Batista and Albin Pinter, *Applied Catalyst A: General*, **347**, 23-33 (2008).
24. G. Carja, L. Dartu, K.Okada and E. Fortunato, *Chemical Engineering Journal*, **222**, 60-66,(, 2013), http://dx.doi.org/10.1016/j.cej.2013.02.039.
25. G. Ren, D.Hu, Eileen W. C Cheng, M. A. Vargas-Reus and P. Reip, *International Journal of Antimicrobial Agents*,**33**, 587-590 (2009), https://doi.org/10.1016/j.ijantimicag.2008.12.004.
26. M.Mousa, A. Hussein, M. Suleiman, B. Hammouti and T. B. Hadda, *Journal of Material Environmental Sciences*, **4**, 792-797 (2013), https://www.researchgate.net/publication/237047396.